Molecular docking, ADME and toxicity study of some chemical and natural plant based drugs against COVID-19 main protease

Kaushik Sarkar
and Rajesh Kumar Das*

Department of Chemistry,
University of North Bengal,
Darjeeling, West Bengal, 734013, India
Email: kaushikchemistry@gmail.com
Email: rajeshnbu@gmail.com
*Corresponding author

Abstract: In view of the non-availability of any secure vaccine for COVID-19 caused by SARS-CoV-2, scientists around the world have been running to develop potential inhibitors against SARS-CoV-2. The present study helps us to identify and screen best phytochemicals (chemical drugs or plant based compounds) as potent inhibitors against COVID-19. In this study, we have measured the virtual interactions of COVID-19 main protease (PDB: 6LU7) with lung cancer, bronchitis and blood thinner drugs as well as some natural plant based compounds. Best docking results have been considered on the basis of disulfiram, tideglusib and shikonin. Absorption, distribution, metabolism and excretion (ADME) and toxicity are also predicted for these compounds. From this study, we will expect these drugs to undergo validation in human clinical trials to use as promising candidates for antiviral treatment with high potential to fight against COVID-19.

Keywords: COVID-19 main protease; lung cancer drugs; bronchitis drug; blood thinner drug; plant based compounds; molecular docking; ADME; toxicity.

Reference to this paper should be made as follows: Sarkar, K. and Das, R.K. (2021) 'Molecular docking, ADME and toxicity study of some chemical and natural plant based drugs against COVID-19 main protease', *Int. J. Computational Biology and Drug Design*, Vol. 14, No. 1, pp.43–63.

Biographical notes: Kaushik Sarkar received his MSc in Chemistry from University of North Bengal (Inorganic specialization) in 2016. After that in the year 2019, he joined the research group of Dr. Rajesh K. Das and he is continuing his research work as junior research fellow from the same institution. His research interests include computer aided drug design.

Rajesh Kumar Das earned his PhD in Chemical Science from the University of North Bengal in 2011. After serving on the faculty at Balurghat College, he moved to University of North Bengal, where he is presently Assistant Professor of Inorganic chemistry. His research encompasses computational approaches towards drug designing. He is a life member of CRSI, Indian Chemical Society and Indian Science Congress. He is a potential reviewer of

Drug Development Research, Coronaviruses, Editorial Board Member of *Drug Design and Medicinal Chemistry*, *Current Chinese Science-Bioinformatics*, Guest Editor of *The Open Microbiology Journal* and Brand Ambassador of Bentham Science Publishers.

1 Introduction

From December 2019, Wuhan in China found many symptoms as a group of pneumonia such as fever, cough, fatigue, shortness of breath due to identification of β- coronavirus (Guan et al., 2020; Wang et al., 2020). Later on 12 January, 2020, WHO declared this virus as 2019 novel corona virus (2019-nCoV) and formally designated as COVID-19 disease (de Wit et al., 2020). On February11, 2020, International Committee of Coronavirus Study Group (CSG) also recommended the name of this virus as SARS-CoV2 (Guo et al., 2020). The first lethal case of this virus was reported on 11 January, 2020. Nowadays, this virus is evolved to other countries all over the world by affecting various patients who have nothing travel history to China (Rothe et al., 2020). Recently, total cases around the world were recorded as 8525042 with 456973 deaths (Situation Report – 152, 2020). The genome of this virus is comprised of approximately 30,000 nucleotides and two of its poly-proteins, pp1a and pp1ab were required for viral replication and transcription (Zhou et al., 2020; Wu et al., 2020). Functional polypeptides are released from Poly-proteins by extensive proteolytic process, especially by 33.8-kDa main protease (M^{pro}). This M^{pro} (key CoV enzyme) is considered as an attractive target for designing new antiviral drug due to the absence of its closely related homologous in humans (Pillaiyar et al., 2016, Anand et al., 2002; Yang et al., 2003).

Because of major outbreak in almost all nations worldwide, this disease approaches researchers for designing promising tool for the discovery of some therapeutic drug candidates against COVID-19. Molecular docking has become now a promising tool for discovery and development of new drug candidate. By using this tool, there is a possibility of molecular interaction of ligand (drug) molecules inside the binding pocket of target protein (receptor) (Mcconkey et al., 2002). It is comprised of the study of all the factors that are being utilised for drug discovery such as identifying hit molecules, optimising lead compound and also virtual screening (Jorgensen, 2004; Bajorath, 2002; Langer and Hoffmann, 2001; Kitchen et al., 2004). This study involves the in silico molecular docking analysis of many synthetic drugs (lung cancer, bronchitis and blood thinner) with some chemical components from natural sources (Ocimum Sanctum, Zingiber officinale, Justicia Adhatoda) against COVID-19 main protease which is provided with proper binding site (PDB: 6LU7).

The asymmetric unit of COVID-19 main protease (M^{pro}) at 2.1Å resolution in complex with N3 contains only one polypeptide. These two asymmetric units, designated as protomer A and B associate to form a dimer and each protomer has three domains (Jin et al., 2020). The asymmetric unit of COVID-19 main protease (PDB: 6LU7) has three domains; I (residues 8–101), II (residues 102–184) and III (residues 201–303) (Jin et al., 2020). The receptor of COVID-19 main protease has a particular substrate-binding

site, located in a cleft between domain I and domain II and suggesting the antiviral inhibitors targeting this site should have higher COVID-19 inhibitory activity (Jin et al., 2020).

2 Materials and methods

2.1 Drug structures

The chemical information of various types of 44 chemical drugs and 10 natural plant based compounds were collected from various databases like Food and Drug Administration (FDA), National Cancer Institute (NIH), Drug Bank, drugs.com and Google search engine. All derivative ligand compounds were drawn using Chem Sketch Tool (ACD/Structure Elucidator, version 2018.1., 2019). The selected compounds having different structures were shown in Figures 1 and 2. Preparation of ligands includes adding all explicit hydrogens, 2D-3D structure conversion. All chemical structures were optimised through Merck Molecular Force Field (MMFF94) under Avogadro suite (Hanwell et al., 2012).

Figure 1 Structure of various chemical drugs

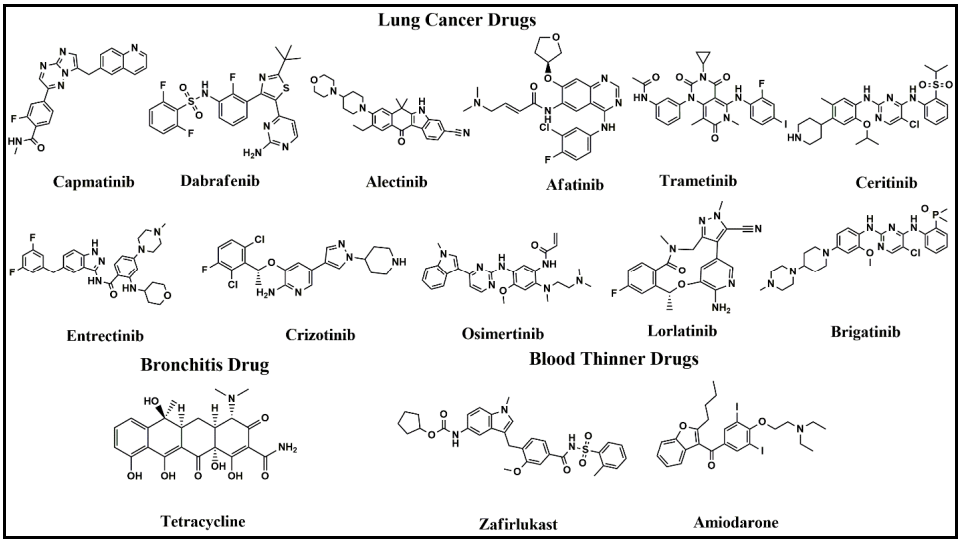

2.2 Receptor preparation

The three dimensional X-ray crystal structure of SARS-CoV-2 virus (COVID-19 main protease) was retrieved from the Protein Data Bank (http://www.rcsb.org/ pdb) (PDB ID: 6LU7). All the ligands and water molecules were removed from the crystal structure of COVID-19 prior to docking using Molegro Molecular Viewer (MMV) 2.5.0 tool (Molegro Molecular Viewer. MMV 2.5.0., 2012).

Figure 2 Structure of various natural plant based compounds

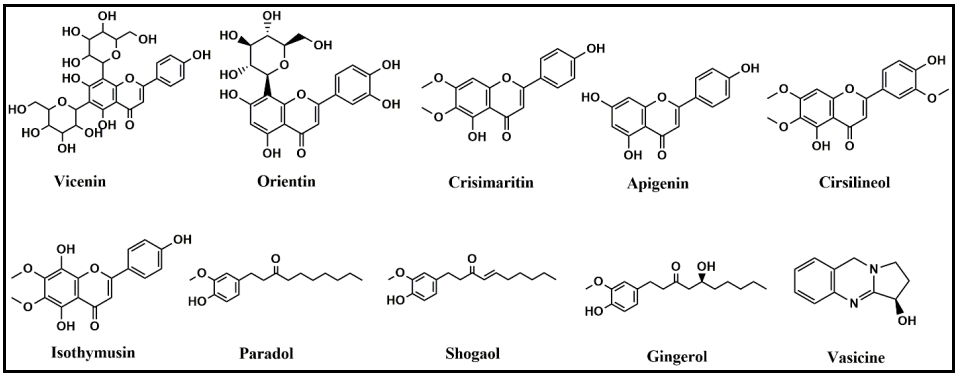

2.3 Molecular docking simulation

The docking protocol, Auto dock 4.2 (ADT 4.2) (Morris et al., 2009) was used to predict the binding mode of drug molecules into the binding site of COVID-19 receptor (PDB ID: 6LU7). The receptor molecule was prepared by checking, repairing missing atoms and adding polar hydrogen with no bond order using graphical user interface of ADT 4.2. The ligands were also prepared as a PDB file from all the optimised Avogadro output to assist the rigid docking process. Active torsions were set to maximum number of atoms. Kollman charges have been assigned to the protein and Gasteiger charges to ligands. The input grid box has size 70, 70, 70 Å (x, y and z respectively) and center at –11.83, 13.187, 68.631 (*x*, *y* and *z* respectively) with spacing 0.375 Å using Auto Grid 4.0, integrated in ADT 4.2. Lamarckian Genetic Algorithm (LGA) was kept as default in all separate molecular docking. The docked models with binding energies were considered for further studies. The results of docked complexes were converted into (pdb) format from (dlg) using PMV 1.5.6 (Sanner, 1999). All docking visualizations were performed using BIOVIA Discovery Studio visualiser (Dassault Systèmes BIOVIA, Discovery Studio Modeling Environment, 2016).

2.4 ADME and toxicity preparation

PreADMET (http://preadmet.bmdrc.org/) server was used to test ADME profiles (Absorption, Distribution, Metabolism, and Excretion) and drug-likeness properties of all drug compounds. Molinspiration (http://www.molinspiration.com) and OSIRIS property explorer (http://www.organic-chemistry.org/prog/peo/) were used to calculate partition coefficient (logP), topological polar surface area (TPSA), molecular weight (MW), drug-likeness, drug-score and number of violation to Lipinski's rule. The overall toxicity of most active derivative compounds was predicted by OSIRIS program as it indicates fragment based properties responsible for mutagenic, tumorigenic, irritant, and reproductive effect.

3 Results

Out of 44 chemical drugs, only 14 have shown higher binding energy with COVID-19 main protease (PDB: 6LU7) compared to disulfiram, tideglusib and shikonin (–5.13, –8.26, –6.67 kcal/mol respectively) (Figure S1–S3 respectively) as proposed by Jin et al. Besides, 10 natural compounds also displayed significant binding energy with COVID-19 receptor. After successful docking of these drugs candidates (ligands) into the COVID-19 main protease, the results found various modes of protein-ligand interactions with the generation of particular docking score i.e., binding energy (ΔG_{bind}). The binding mode with highest negative binding energy is considered as best mode of binding due to its most stability for that ligand. The highest binding energy which indicates better fit for all the drug is summarised in Table 1. It also found the interaction of specific amino acid taking part in the protein-ligand interactions.

Table 1 Target (protein) and the drug candidates (ligands) undergoing docking experiment with their best docking score (highest negative binding energy) and various type of interactions

Compound	*van der Waals interaction*	*H-bond interaction*	*Number of H-bond*	ΔG_{bind} (kcal/mol)
Capmatinib	Arg188, Leu167, His163, His172, Ser144, Glu166, His164	Gln192	1	–10.59
Dabrafenib	Ser144, Leu141, His163, His172, Met49, His164, Arg188, Asp187, Leu167, Gln192, Ala191, Gly143	Glu166, Thr190	2	–9.82
Alectinib	Gln192, Leu167, Arg188, Asp187, His164, Met49, Leu27, Thr26, Asn142, Glu166, Thr190, Ala191	Cys145	1	–9.79
Afatinib	Ser144, Leu141, Phe140, His172, His164, Val186, Gln192, Thr190, Pro168, Arg188, Asp187, Tyr54	Gly143, Glu166	2	–9.75
Trametinib	Thr190, Leu167, Arg188, Asp187, Tyr54, Ser144, Asn142, Thr25	Gln192, His164, Gly143	3	–9.74
Ceritinib	Pro168, Thr190, Gln192, Arg188, Met49, His164, His41, Val42, Thr25, Leu27, Gly143, Ser144, His163, Phe140, Leu141, His172, Leu167	Glu166, Thr26, Asn142	3	–9.34
Brigatinib	Pro168, Gln189, Arg188, Ser144, His172, Gly143, Leu141, Met49, Thr25, Leu27, Asn142	Glu166, Thr190, Gln192	3	–8.66
Crizotinib	Gln192, Asn142, Leu1414, His172, His163, Pro168, Ala191, Leu167	Thr190, Arg188, Phe140	3	–8.60

Table 1 Target (protein) and the drug candidates (ligands) undergoing docking experiment with their best docking score (highest negative binding energy) and various type of interactions (continued)

Compound	*van der Waals interaction*	*H-bond interaction*	*Number of H-bond*	ΔG_{bind} (kcal/mol)
Orlatinib	Gln189, His164, Met49, Gly143, His163, Asn142, His172	Glu166, Cys145, Ser144, Leu141	5	–8.56
Osimertinib	Asp187, Arg188, Gln192, Thr190, Gly170, Leu141, His164	Glu166, Leu167	2	–8.42
Entrectinib	Gly143, Ser144, Leu41, Phe140, His163, His172, Pro52, Tyr54, Arg188, His164, Thr190, Gln192	No	No	–9.13
Tetracycline	Asp187, Arg188, Gln189, Leu167	Phe140, Asn142, Glu166, His164	8	–9.04
Amiodarone	Leu141, Thr190, Gln192, Asp187, Tyr54, His164, Ser144	Arg188	1	–8.47
Zafirlukast	Gln189, Asn142, Leu141, Leu27, Thr26, Thr25, Met49, Leu167	Ser144, Cys145, Gly143	4	–9.81
Vicenin	Leu141, Phe140, Gly143, His172, Thr25, Thr26, Leu27, Ala191	Arg188, Thr190, Gln192, Glu166, Gln189, Asn142	11	–8.19
Orientin	Leu167, His164, Gln189, Gln192,	Pro168, Glu166, Arg188, Thr190, Gly170	7	–7.95
Cirsimaritin	Ala191, Gln192, Leu167, Pro52, Arg188, Asp187, Tyr54, Glu166	Thr190, His164	2	–7.65
Apigenin	Ala191, Leu167, Gln192, Arg188, Tyr54, Pro52, Cys145, Glu166	Thr190, Asp187, His164	3	–7.56
Cirsilineol	Asn142, Pro168, Thr190, Leu167, Gln192, His164	Cys145, Gly143, Leu141, Ser144, Arg188	5	–7.45
Isothymusin	Leu167, Thr190, His164, Met49, His41, Asp187, Arg188	Gln192, Glu166, Cys145	3	–7.14
Paradol	Asp187, His164, Ala191, Gln192, Leu167, Arg188	Glu166, Thr190	2	–6.63
Shogaol	Phe140, His163, Pro52, Arg188, His164, Asp187, Tyr54, Gln189, Asn142	Glu166, Leu141, Ser144, Cys145, Gly143	5	–6.61
Gingerol	His41, Cys44, Asp187, Tyr54, Ala191, Cys145	His164, Gln192, Thr190, Glu166	4	–6.12
Vasicine	Met49, Asp187, Gln189, Gln192	Arg188	1	–6.08

3.1 Visualisation of docking results

Lung cancer drugs namely capmatinib, dabrafenib, alectinib, afatinib, trametinib, ceritinib, entrectinib, brigatinib, crizotinib, lorlatinib and osimertinib were docked with COVID-19 main protease, showing higher binding energies of –10.59, –9.82, –9.79, –9.75, –9.74, –9.34, –9.13, –8.66, –8.60, –8.56 and –8.42 kcal/mol respectively, when compared with disulfiram, tideglusib and shikonin (–5.13, –8.26 and –6.67 kcal/mol respectively) as proposed by Jin et al. (Table S2). Tetracycline (a bronchitis drug), amiodarone and zafirlukast (blood thinner drugs) have also shown higher binding energy of –9.04, –8.47 and –9.81 kcal/mol respectively. Similarly, plant based compounds (ligand) orientin, vicenin, cirsimartin, cirsilineol, apigenin, isothymusin, shogaol, paradol, gingerol and vasicine have shown the binding value of –7.95, –8.19, –7.65, –7.45, –7.56, –7.14, –6.61, –6.63, –6.12 and –6.08 kcal/mol respectively. Herein, results showed that six ligands, orientin, vicenin, cirsimartin, cirsilineol, apigenin, isothymusin have displayed higher binding affinity than shikonin (–6.67 kcal/mol) and disulfiram (–5.13 kcal/mol). Besides, other four ligands, shogaol, paradol, gingerol and vasicine have high binding affinity than disulfiram (–5.13 kcal/mol) only. The amino acids taking part in the protein-ligand interaction is shown with ligands as blue colour stick with amino acids (yellow sticks) surrounding them. The interaction shown by green dash lines refers to the hydrogen bonding interactions between the protein and ligand.

3.2 Visualisation of ADME and toxicity

Here toxicity and ADME prediction were done with compounds which have significant binding affinity with COVID-19 receptor. It was shown from Table 2 that most of the compounds used in this study were successfully qualified the Lipinski, s rule of five (Rastogi et al., 2015) (except dabrafenib, ceritinib, amiodarone, zafirlukast, vicenin and orientin). Except few of them, most of these compounds were predicted to have good oral bioavailability (Table 3). A large number of compounds have shown excellent permeability, while few have relatively less or poor permeability (Table 3). The drug score and drug-likeness values of the ligands were also predicted (Table 4). It was revealed from the data that all these compounds have significant drug score value in the range of 0.1–1.0.

Toxicity effect can predict the fate of a promising drug. It had been shown that drug molecules having low toxicity/side effect contain the high order of therapeutic index (Tamargo et al., 2015). So toxicity prediction was done for all the derived compounds using OSIRIS Property Explorer (Table 4). It was noted that all the derived compounds, except few of them have low toxicity. The toxicity parameters were used in OSIRIS as colour codes, as usual green stands for low, yellow stands for mediocre and red stands for high toxicity.

4 Discussions

4.1 Molecular docking study

After successful docking of all the ligands employed in these docking experiments, the results showed significant binding of the ligands with the COVID-19 main protease. The

binding site of COVID-19 main protease is composed of such amino acids His141, Ser46, Met49, Tyr54, Phe140, Leu141, Asn142, Gly143, Cys145, His163, His164, Met165, Glu166, Leu167, Pro168, His172, Phe185, Asp187, Gln189, Thr190, Ala191 and Gln192 (Jin et al., 2020). All the chemical and natural compounds having appropriate binding energies into the binding site of COVID-19 main protease are shown in Figure 3.

Table 2 Druglikeness and ADME properties of various compounds

Compound		*Rule of five*	*BBB*	*HIA%*	*PPB%*
Chemical Drugs	Capmatinib	Suitable	0.03	96.68	90.94
	Dabrafenib	Violated	0.02	96.66	89.57
	Alectinib	Suitable	4.25	95.33	85.65
	Afatinib	Suitable	0.19	95.90	79.51
	Trametinib	Suitable	0.04	97.76	85.25
	Ceritinib	Violated	1.87	95.29	86.61
	Brigatinib	Suitable	0.08	96.28	80.96
	Crizotinib	Suitable	0.06	95.91	86.28
	Lorlatinib	Suitable	0.11	97.55	82.77
	Osimertinib	Suitable	0.18	96.35	85.18
	Entrectinib	Suitable	1.92	93.13	81.99
	Tetracycline	Suitable	0.03	35.22	33.21
	Amiodarone	Violated	2.49	97.51	91.95
	Zafirlukast	Violated	0.02	97.17	97.17
Natural plant based compounds	Vicenin	Violated	0.03	1.95	38.10
	Orientin	Violated	0.03	14.99	63.12
	Cirsimaritin	Suitable	0.06	7.45	88.06
	Apigenin	Suitable	0.57	88.12	97.25
	Cirsilineol	Suitable	0.03	93.45	85.58
	Isothymusin	Suitable	0.08	87.82	87.10
	Paradol	Suitable	4.22	95.08	100.0
	Shogaol	Suitable	4.26	95.18	100.0
	Gingerol	Suitable	1.47	91.72	100.0
	Vasicine	Suitable	0.54	95.47	80.33

4.1.1 Docking study of chemical compounds

4.1.1.1 Docking study of lung cancer drugs

Capmatinib docked in COVID-19 main protease, showed highest binding affinity of –10.59 kcal/mol. The interaction of capmatinib with the protease (Figure 4) showed a high affinity interaction into the binding pocket region of the protease. The docking study of capmatinib is further evidenced by hydrogen bonding between the oxygen of the carbonyl group (amide side chain) of capmatinib with Gln192. Some of the van der Waals interactions of capmatinib with His164, Glu166, His163, His172, Ser144, Arg188 and Leu167 have been observed. The docking of dabrafenib with the COVID-19 main

protease revealed that it showed high affinity interaction with the protein, having affinity of –9.82 kcal/mol (Figure 5). The interaction results in the form of two hydrogen bonds between dabrafenib and amino acid residues Glu166 and Thr190 of the protein. The fluorine atom (benzene ring) shows significant hydrogen bonding with Glu166 and the other one is shown by hydrogen atom of amine group and Thr190. The tertiary butyl group shows π-σ interaction with His41. The docking of alectinib docked in COVID-19 main protease shows significant interaction in the binding site with the affinity of –9.79 kcal/mol (Figure 6). The major interaction between alectinib and the protease is characterised by hydrogen bonding between the oxygen atom of carbonyl group and Cys145. Some of the π-σ and π-π interactions have been observed between alkyl side chain and aromatic ring and His41 respectively. Results obtained by docking of afatinib docked in COVID-19 main protease showed the binding affinity of –9.75 kcal/mol (Figure 7). It shows significant binding with two hydrogen bonds between, two oxygen atoms of tetrahydrofuran ring and carbonyl group (hydrocarbon chain) with Gly143 and Glu166 respectively. The π-π and π-σ interactions have also been observed between benzene and quinoline rings with Gln189 and His41 respectively.

Table 3 Molecular descriptor properties of various compounds

Compound	*miLogP*	*TPSA*	*natoms*	*MW*	*nON*	*nOHNH*	*nviolations*	*nrotb*	*volume*
Capmatinib	3.20	85.08	31	412.43	7	1	0	4	353.27
Dabrafenib	4.72	110.9	35	519.57	7	3	1	6	412.62
Alectinib	5.28	72.36	36	482.63	6	1	1	3	456.53
Afatinib	4.21	88.61	34	485.95	8	2	0	8	417.87
Trametinib	4.12	107.1	37	615.40	9	2	1	5	445.89
Ceritinib	6.17	105.2	38	558.15	8	3	2	9	499.36
Brigatinib	5.06	85.86	40	584.11	9	2	2	8	528.37
Crizotinib	4.01	78.00	30	450.35	6	3	0	5	375.18
Lorlatinib	1.73	110.1	30	406.42	8	2	0	0	350.22
Osimertinib	4.08	87.55	37	499.62	9	2	0	10	470.39
Entrectinib	5.65	85.52	41	560.65	8	3	2	7	502.81
Tetracycline	–0.24	181.6	32	444.44	10	7	1	2	377.44
Amiodarone	8.31	42.68	31	645.32	4	0	2	11	437.04
Zafirlukast	5.69	115.7	41	575.69	9	2	2	9	508.07
Vicenin	–2.1	271.2	42	594.52	15	11	3	5	486.36
Orientin	0.03	201.3	32	448.38	11	8	2	3	363.22
Cirsimaritin	2.60	98.37	25	344.32	7	2	0	4	292.67
Apigenin	2.46	90.89	20	270.24	5	3	0	1	224.05
Cirsilineol	2.60	98.37	25	344.32	7	2	0	4	292.67
Isothymusin	2.69	109.4	24	330.29	7	3	0	3	275.14
Paradol	4.60	46.53	20	278.39	3	1	0	10	287.57
Shogaol	4.35	46.53	20	276.38	3	1	0	9	281.38
Gingerol	3.22	66.76	21	294.39	4	2	0	10	295.61
Vasicine	1.04	35.83	14	188.23	3	1	0	0	173.66

Table 4 Fragment-based drug-likeness and toxicity properties of various compounds using OSIRIS

Compound		*Mutagenic*	*Tumorigenic*	*Irritant*	*Reproductive effective*	*cLogP*	*Druglikeness*	*Drug Score*
Chemical drugs	Capmatinib	Red	Green	Green	Red	2.30	4.52	0.28
	Dabrafenib	Green	Green	Green	Green	4.54	–3.50	0.17
	Alectinib	Green	Green	Green	Green	4.77	–0.06	0.28
	Afatinib	Green	Green	Green	Green	3.64	–4.11	0.24
	Trametinib	Green	Green	Green	Green	3.64	4.93	0.29
	Ceritinib	Green	Green	Green	Green	6.26	1.32	0.19
	Brigatinib	Red	Yellow	Red	Yellow	4.45	–7.29	0.04
	Crizotinib	Green	Green	Green	Green	3.54	3.12	0.52
	Lorlatinib	Green	Green	Green	Green	1.20	1.04	0.59
	Osimertinib	Red	Yellow	Yellow	Yellow	3.42	–4.58	0.09
	Entrectinib	Green	Green	Green	Green	4.20	1.51	0.30
	Tetracycline	Green	Green	Green	Red	–1.26	5.59	0.49
	Amiodarone	Green	Green	Red	Green	6.28	4.26	0.11
	Zafirlukast	Green	Green	Green	Green	5.67	–7.90	0.12
Natural plant based compounds	Vicenin	Red	Green	Green	Yellow	–2.49	–1.26	0.18
	Orientin	Red	Green	Green	Green	–0.42	–0.71	0.32
	Cirsimaritin	Red	Yellow	Green	Green	2.47	1.24	0.36
	Apigenin	Red	Green	Green	Green	2.34	1.21	0.47
	Cirsilineol	Red	Yellow	Green	Green	2.47	1.24	0.36
	Isothymusin	Red	Red	Green	Green	2.20	1.06	0.27
	Paradol	Green	Green	Green	Green	4.59	–20.3	0.35
	Shogaol	Green	Green	Green	Green	4.33	–14.5	0.37
	Gingerol	Green	Green	Green	Green	3.56	–7.78	0.40
	Vasicine	Green	Green	Green	Green	0.22	3.95	0.96

The interaction of trametinib with the protease (Figure 8) showed binding affinity of –9.74 kcal/mol. This is further evidenced by hydrogen bonding between the oxygen of the $–NHCOCH_3$ group (side chain of benzene) of trametinib with Gln192, fluorine atom of benzene ring with Gly143 and hydrogen of secondary amine with His164. Amino acid residues Leu167, Arg188, Asp187, Tyr54, Ser144, Asn142, Thr25 and Thr190 have participated towards van der Waals interaction with trametinib. Some of the π-π interaction has been observed between His41of the protein and benzene ring of trametinib. Results obtained by docking of ceritinib docked in COVID-19 main protease showed the binding affinity of –9.34 kcal/mol (Figure S4). It shows significant binding with three hydrogen bonds between, hydrogens of secondary amine (connected through two benzene rings) and Glu166 and Asn142, hydrogen of –NH group (attached to pyrole ring) and Thr26. The docking of entrectinib was also performed with COVID-19 main

protease and showed significant binding affinity affinity of –9.13 kcal/mol (Figure S5). The interaction is primarily characterised by π-σ interaction between the entrectinib with His41. Brigatinib, crizotinib, Lorlatinib and osimertinib also displayed higher binding energy of –8.66, –8.60, –8.56 and –8.42 kcal/mol respectively with the interaction of various amino acid residues of the receptor (Figures S6 and S7).

Figure 3 (a) Surface representation of COVID-19 main protease with all the best fitted ligands. Grey surface represents the receptor and yellow sticks represent ligands and (b) cartoon representation of COVID-19 main protease (green ribbon) with all the ligands (yellow stick) into binding site (see online version for colours)

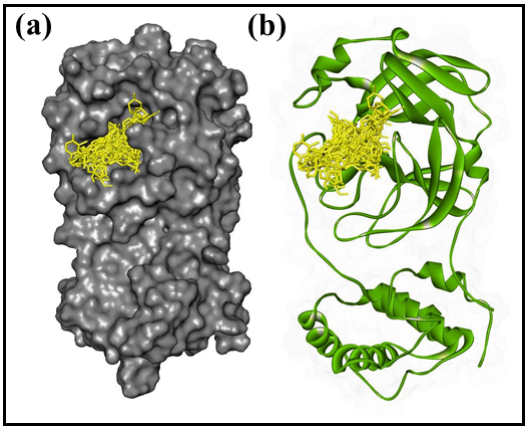

Figure 4 Capmatinib docked in COVID-19 main protease (PDB: 6LU7) with (a) 3D binding mode interaction into the binding pocket of receptor (ligand as blue colour stick and amino acids as yellow) and (b) 2D binding interaction of capmitinib with different amino acids of the receptor (hydrogen bond is shown as deep green dash line) (see online version for colours)

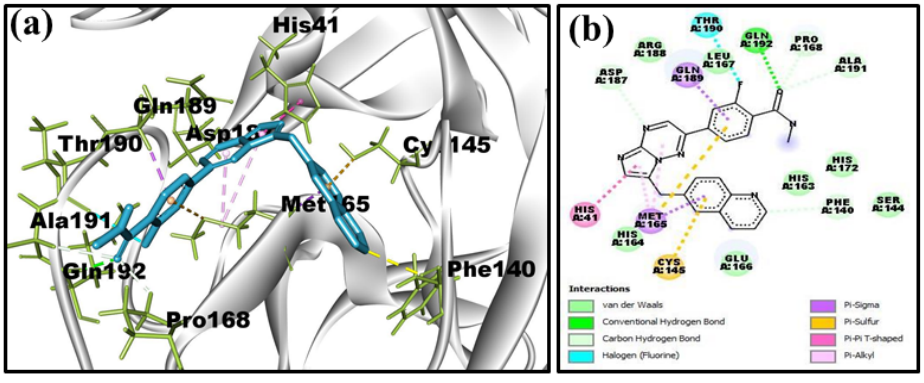

4.1.1.2 Docking study of bronchitis drug

With eight hydrogen bonds, tetracycline (a bronchitis drug) showed promising activity with the protease of COVID-19 with the affinity of –9.04 kcal/mol (Figure 9). Thus this interaction results in eight hydrogen bonds, hydrogen of amide group with Phe140 and Glu166. Similarly other hydrogen bonds are formed by the participation of various

hydroxyl groups of the ligand with Asn142, His164 and also Glu166. An unfavourable donor-donor interaction has also been observed between hydrogen of hydroxyl group (attached to benzene ring) and Cys145. Since this binding is characterised by eight hydrogen bonds, the interaction can be recognised as possible mode of binding of tetracycline with the protease of COVID-19.

Figure 5 Dabrafenib docked in COVID-19 main protease (PDB: 6LU7) with (a) 3D binding mode interaction into the binding pocket of receptor (ligand as blue colour stick and amino acids as yellow) and (b) 2D binding interaction of dabrafenib with different amino acids of the receptor (hydrogen bonds are shown as deep green dash line) (see online version for colours)

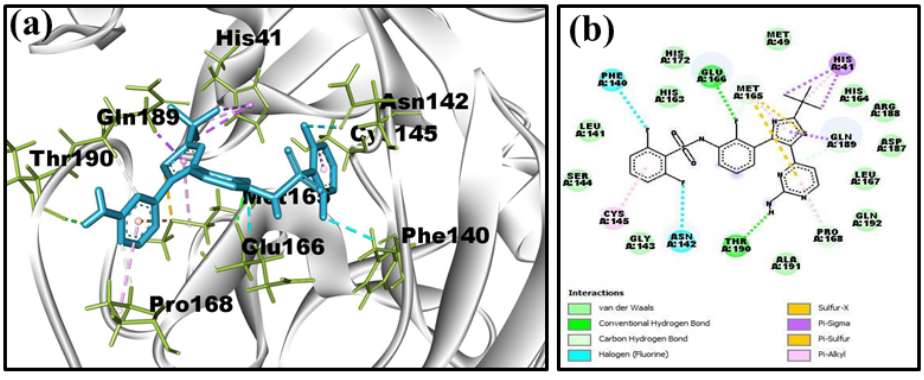

Figure 6 Alectinib docked in COVID-19 main protease (PDB: 6LU7) with (a) 3D binding mode interaction into the binding pocket of receptor (ligand as blue colour stick and amino acids as yellow) and (b) 2D binding interaction of alectinib with different amino acids of the receptor (hydrogen bond is shown as deep green dash line) (see online version for colours)

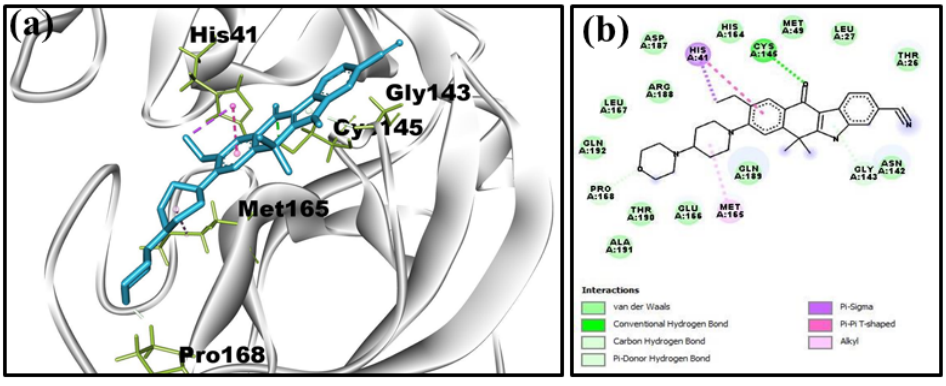

4.1.1.3 Docking study of blood thinner drug

Zafirlukast and amiodarone (two blood thinner agents) also showed promising activity with the protease of COVID-19 with the affinity of –9.81 and –8.47 kcal/mol. The interaction of zafirlukast results in forming five hydrogen bonds, between carbonyl and sulphonyl oxygen with Ser144, Cys145 and Gly143 amino acid residues of the protein (Figure 10). Similarly amiodarone found one hydrogen bond with the participation of

oxygen atom of furan ring with Arg188 (Figure S8). Since the binding for zafirlukast is characterised by five hydrogen bonds, this interaction can be considered as possible mode of binding with the protease of COVID-19.

Figure 7 Afatinib docked in COVID-19 main protease (PDB: 6LU7) with (a) 3D binding mode interaction into the binding pocket of receptor (ligand as blue colour stick and amino acids as yellow) and (b) 2D binding interaction of afatinib with different amino acids of the receptor (hydrogen bonds are shown as deep green dash line) (see online version for colours)

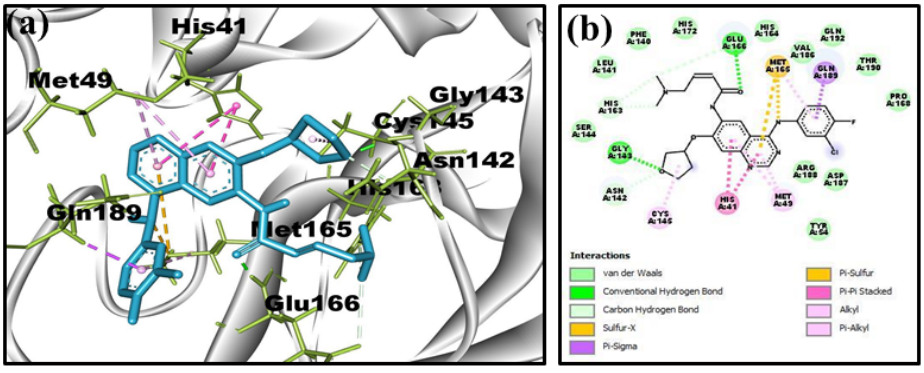

Figure 8 Trametinib docked in COVID-19 main protease (PDB: 6LU7) with (a) 3D binding mode interaction into the binding pocket of receptor (ligand as blue colour stick and amino acids as yellow) and (b) 2D binding interaction of trametinib with different amino acids of the receptor (hydrogen bonds are shown as deep green dash line) (see online version for colours)

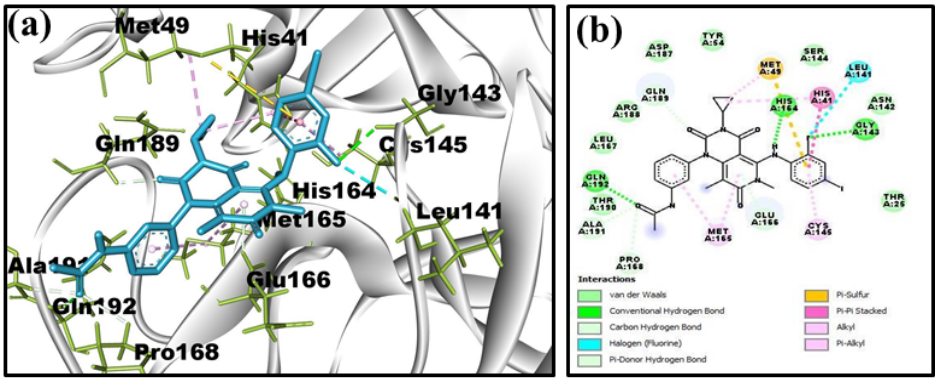

A common feature was observed throughout this analysis for all ligands. In most of the ligand the Gln192, Glu166, Thr190, Cys145 & Gly143 residues were common which are involved in H-bond interactions. $-SO_2$ containing ligands with a large number of benzene rings showed a higher binding energy of interaction. Similarly, compounds containing fluoro, choloro, or iodo (more electronegative) substituents were found to be very effective in forming high binding affinity. All nitrogenous based compounds with amide or substituted amide groups showed a high affinity of the interaction. Besides, highly polar hydroxyl groups formed a higher number of H-bonds (5 H-bonds) found in the case of tetracycline.

Figure 9 Tetracycline docked in COVID-19 main protease (PDB: 6LU7) with (a) 3D binding mode interaction into the binding pocket of receptor (ligand as blue colour stick and amino acids as yellow) and (b) 2D binding interaction of tetracycline with different amino acids of the receptor (hydrogen bonds are shown as deep green dash line) (see online version for colours)

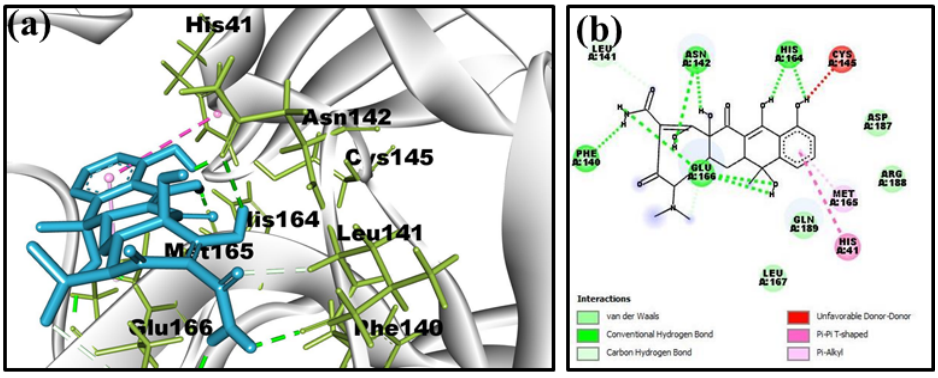

Figure 10 Zafirlukast docked in COVID-19 main protease (PDB: 6LU7) with (a) 3D binding mode interaction into the binding pocket of receptor (ligand as blue colour stick and amino acids as yellow) and (b) 2D binding interaction of zafirlukast with different amino acids of the receptor (hydrogen bonds are shown as deep green dash line) (see online version for colours)

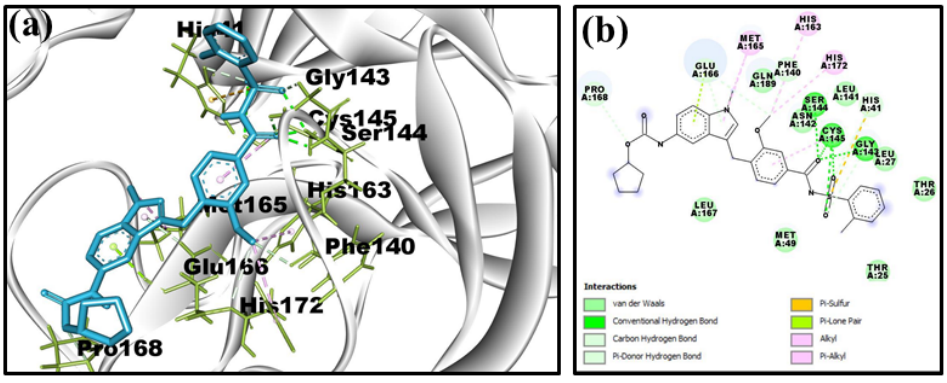

4.1.2 Docking study of plant based compounds

Due to the formation of eleven hydrogen bonds, vicenin (a natural compound from ocimum sanctum) showed promising binding activity with the protease of COVID-19 with the affinity of –8.19 kcal/mol (Figure S9). These interaction results eleven hydrogen bonds formed by the participation of hydrogen and oxygen atoms of hydroxyl groups with amino acids Arg188, Thr190, Gln192, Glu166, Gln189 and Asn142. Some of the van der Waals interactions of vicenin with Leu27, Thr26, Thr25, His163, His172, Gly143, Phe140 and Leu141 have also been observed. Since the binding is characterised by highest number of hydrogen bonds, this interaction can be considered as possible mode of binding of tetracycline with the protease of COVID-19. Orientin also showed promising activity with the protease of COVID-19 with the affinity of –7.95 kcal/mol (Figure S10). This interaction results in forming seven hydrogen bonds, hydrogen and

oxygen of hydroxyl group (connected to benzene ring) with Pro168, Glu166, Gly170 and Arg188. Amino acid Thr190 also formed the remaining hydrogen bond with the ligand. An unfavourable acceptor-acceptor bond is formed by hydroxyl oxygen with Arg188. Results obtained from docking of cirsimartin with the protease of COVID-19 have shown the binding affinity value of –7.65 kcal/mol (Figure 11). This interaction results in forming only two hydrogen bonds, hydrogen of hydroxyl group (connected to benzene ring) with Thr190 and His164. An unfavourable donor-donor interaction is found between hydroxyl hydrogen with Cys145.

Figure 11 Cirsimartin docked in COVID-19 main protease (PDB: 6LU7) with (a) 3D binding mode interaction into the binding pocket of receptor (ligand as blue colour stick and amino acids as yellow) and (b) 2D binding interaction of cirsimartin with different amino acids of the receptor (hydrogen bonds are shown as deep green dash line) (see online version for colours)

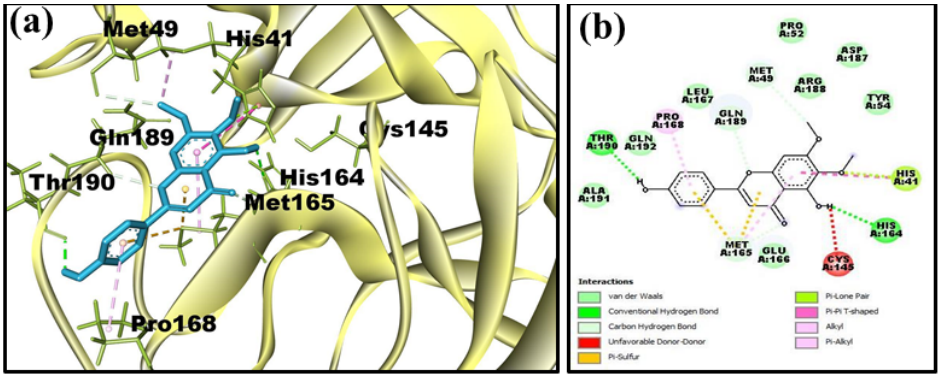

On the other hand apigenin, cirsilineol and isothymusin also docked into the binding site of COVID-19 main protease with binding affinity value of –7.56, –7.45 and –7.14 respectively. Apigenin formed three hydrogen bonds by the participating hydrogen atom of –OH group (attached to benzene ring) with Thr190, Asp187 and His164 (Figure S11). The pi-pi interaction is formed between benzene ring with His41. Cirsilineol formed four hydrogen bonds with the protein. Ser144, Leu141, Gly143, Cys145 and Arg188 are participated in forming these hydrogen bonding interactions (Figure S12). Similarly, amino acid residues Glu166, Gln192 and Cys145 are participated in forming three hydrogen bonds with isothymusin (Figure S13). The interaction of paradol (from Zingiber officinale) with the protease (Figure 12) showed binding affinity of –6.63 kcal/mol. This is further supported by hydrogen bonding between the oxygen of the carbonyl group (attached to hydrocarbon chain) of trametinib with Glu166, hydrogen of –OH group (benzene ring) with Thr190. Amino acids Asp187, His164, Arg188, Gln189, Leu167, Gln192 and Ala191 have participated towards van der Waals interaction with paradol. With five hydrogen bonds, shogaol from natural component also found promising activity with the protease of COVID-19 with the affinity of –6.61 kcal/mol (Figure S14). Thus this interaction results in five hydrogen bonds, oxygen of carbonyl of hydrocarbon chain with Glu166, hydrogen of –OH group and oxygen of $–OCH_3$ group (connected to benzene ring) with Leu141, Ser144, Cys145 and Gly143 respectively. A π-σ interaction has also been observed between hydrocarbon chain and His41. Gingerol also found four hydrogen bonding interactions into the binding site of COVID-19 main

protease, having binding affinity of –6.12 kcal/mol. Amino acid residues Gln192, Thr190, His164 and Glu166 are participated in forming these four hydrogen bonds (Figure S15).

Figure 12 Paradol docked in COVID-19 main protease (PDB: 6LU7) with (a) 3D binding mode interaction into the binding pocket of receptor (ligand as blue colour stick and amino acids as yellow) and (b) 2D binding interaction of paradol with different amino acids of the receptor (hydrogen bonds are shown as deep green dash line) (see online version for colours)

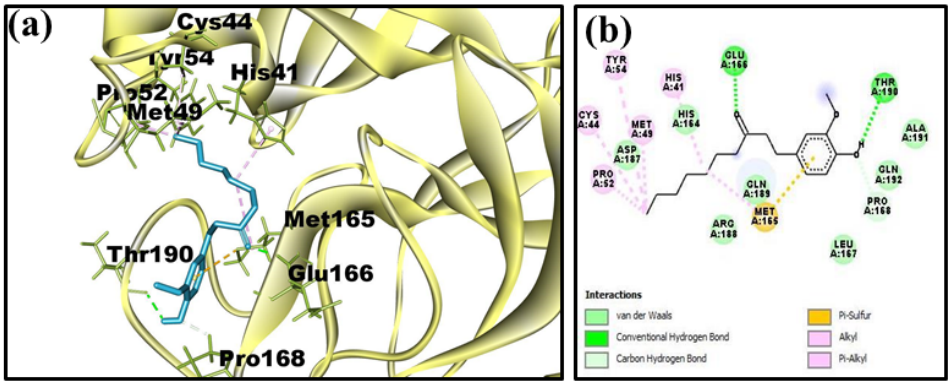

Ligands with decane-3-one substituent (paradol) showed high binding affinity than the other two ligands i.e., decane-3-one substituent with alkene (shogaol) or hydroxyl group (gingerol) due to the decrease of electron affinity of carbonyl group in the presence of alkene or hydroxyl group. One common residue Glu166 was found for all these three ligands in forming H-bond interaction with the oxygen atom of the carbonyl group (present in alkane side chain). On the other hand, a higher number of H-bond interactions were formed by two ligands namely vicenin & orientin due to the presence of more polar hydroxyl substituents and thus also satisfied considerable binding energy. Besides, aromatic rings with various positions of highly polar hydroxyl and methoxy groups also showed significant binding affinity (crisimartin, apegenin & cirsilineol).

4.2 ADME and toxicity discussion

Table 2 illustrate the in silico ADME properties. Most important parameters used for pharmacokinetic study of a drug are absorption, distribution, metabolism and excretion (Lee et al., 2003). In silico ADME properties of most of these compounds have shown satisfactory result. In silico drug like properties, bioactive score as COVID-19 inhibitor were predicted here to select best drug candidates using OSIRIS suite and Molinspiration online property toolkit. Mutagonic, tumorigenic, irritant, reproductive index and drug-like, drug score values were visualised from OSIRIS and on the other side, Molinspiration predicts such valuable parameters like miLogP, TPSA, number of rotatable bonds (nrotb), number of hydrogen bond acceptors (nON) and donors (nOHNH). Good permeability across cell membrane is based on miLogP parameter. The tendency of generating hydrogen bond prediction is based on TPSA. Number of rotatable bonds denotes the flexibility of the compound. Molecular properties and structural features irrespective of known drugs were checked on the basis of drug-likeness data of

molecules (Lipinski et al., 2001). According to Lipinski's rule of five, compounds having number of violation, nviolations ≤ 1 have shown good bioavailability and here most of the compounds may act as good bioavailable drug. Molecules having miLogP ≤ 5, nOHNH ≤ 5 and nON ≤ 10 are indicated higher probability of solubility in cellular membranes and half of these derived compounds have followed this rule (Husain et al., 2016).

4.2.1 For chemical compounds

According to ADME drug-likeness prediction, only four chemical compounds namely dabrafenib, ceritinib, amiodarone and zafirlukast were violated from rule of five parameters. In this present work, all these chemical compounds (except tetracycline) have better result for intestinal absorption (HIA) closed to 100. Out of these, trametinib containing highest value of HIA (97.76%) has displayed maximum absorption. Results having in vivo blood brain barrier (BBB) penetration indicate that most of the compounds (except alectinib, ceritinib and amiodarone) have low absorption into central nervous system (CNS), less capability to cross CNS. All these compounds containing plasma protein binding data PPB > 80% (except tetracycline drug; 33.21%) indicate strong bound capacity, high skin permeability. Thus from overall results, we may concluded that most of these chemical compounds have capability of good drug likeness and ADME properties. Besides, all nine ligands have shown good partition coefficient (miLogP) values which were in the acceptable range (–0.2 to 5.0). In this study, five chemical compounds (Ceritinib, brigatinib, entrectinib, amiodarone and zafirlukast) have shown much more violations (nviolations = 2) from Lipnski's rule of five. This is due to the molecules having large chemical structure with MW > 500 and low solubility (miLogP > 5).

The in silico toxicity profiling was carried out for all ligands by OSIRIS. It is depending on four toxicity risk type parameters i.e., mutagenicity, tumorigenicity, irritating and reproductive effect by colour codes of red (high), yellow (mediocre) and green (low) (Table 4). Capmatinib, brigatinib and osimertinib were to be non-mutagenic. Similarly, Brigatinib and amiodarone were non-irritant; capmatinib and tetracycline were come out as lowest reproductive effective. Furthermore, drug score value combines druglikeness, cLogP, MW and toxicity risks in one parameter to judge the overall potent qualification of a drug. Here, all chemical ligands have acceptable range of drug score value (0.1 to 0.6).

4.2.2 For natural plant based compounds

In this study, only two natural compounds namely vicenin and orientin were violated from rule of five and also having low absorptivity into human intestine, indicating very low HIA value. These two compounds also have low PPB value, denoting low bound capacity with low skin permeability. On the other hand, crisimartin also displayed low absorption. Here in vivo BBB penetration of paradol and shogaol (BBB > 4) indicate high absorption into CNS. Due to capable of high molecular structure, vicenin and orientin have shown nviolations≥2 from Lipinski's rule of five. The optimum range of mutagenic capacity was exceeded by six ligands (Vicenin, orientin, cirsimaritin, Apigenin, cirsilineol and isothymusin) whereas isothymusin has high risk of irritating effect.

The need of this study is to find a cure therapy for COVID-19 virus by repurposing of many chemical and natural compounds in this dreadful viral outbreak situation. Some medical guidelines are being advised to be given the hydroxychloroquine and azithromycin complex for affected case of emergency. Though this complex may be potent, but adverse side effect bring very alarming condition for the patients. Hence we need to bring equally or more effective alternatives in the form of chemical drug with little or no side effect and also natural plant based compounds (Enmozhi et al., 2020). The plant based drugs are used as very essential potent inhibitor as they are much safe with no known side effects (Enmozhi et al., 2020). Here we found some chemical drugs such as lung cancer, bronchitis and blood thinner as alternative use of COVID-19 inhibitor. Fourteen of them are successfully docked against inhibitor region of COVID-19 main protease showed higher binding affinity when compared to disulfiram, tideglusib and shikonin –5.13, –8.26, –6.67 kcal/mol respectively as proposed by Jin et al. Besides, some natural plant based compounds such as orientin, vicenin, cirsimartin, cirsilineol, apigenin, isothymusin, shogaol, paradol, gingerol and vasicine also found to satisfy comparable binding affinity when docked against the receptor of COVID-19 main protease.

5 Conclusion

The present study was carried out for discovering small molecule inhibitors that could inhibit SARS-CoV2 by binding to the M^{pro} target. Virtual screening was carried out with chemical and plant based compounds. Several ligands showed satisfying binding affinity of interaction. Among them, chemical compounds such as capmatinib, dabrafenib, alectinib, afatinib, trametinib, crizotinib, lorlatinib, osimertinib and tetracycline came out as effective inhibitors based on overall docking, ADME and toxicity parameters. Similarly, paradol, gingerol and vasicine were those natural compounds which passed the overall ADME, toxicity and acceptable binding affinities. Thus, the result of this present work expects further testing of these inhibitors for in vivo and in vitro analysis against COVID-19.

Acknowledgements

We are thankful to UGC, New Delhi for fellowship vide UGC-Ref. No.: 175/(CSIR-UGC NET DEC, 2018). Authors are thankful Department of Chemistry, University of North Bengal, for various supports and also thankful to all Indian people for giving golden opportunity to do this wonderful research.

Conflicts of interest

The authors declare no conflict of interest.

Supplementary material is available on request from the corresponding author, Rajesh Kumar Das.

References

ACD/Structure Elucidator, version 2018.1. (2019) Advanced Chemistry Development, Inc., Toronto, ON, Canada, www.acdlabs.com

Anand, K., Palm, G.J., Mesters, J.R., Siddell, S.G., Ziebuhr, J. and Hilgenfeld, R. (2002) 'Structure of coronavirus main proteinase reveals combination of a chymotrypsin fold with an extra alpha-helical domain', *EMBO J*, Vol. 21, No. 13, pp.3213–3224, doi: 10.1093/emboj/cdf327.

Bajorath, J. (2002) 'Integration of virtual and high-throughput screening', *Nat Rev Drug Discov*., Vol. 1, pp.882–94.

Dassault Systèmes Biovia (2016) *Discovery Studio Modeling Environment, Release 2017*, Dassault Systèmes, San Diego.

de Wit, E., van Doremalen, N., Falzarano, D. and Munster, V.J. (2020) 'SARS and MERS: recent insights into emerging coronaviruses', *Nature Reviews Microbiology*, Vol. 14, pp.523–534, https://doi.org/10.1038/nrmicro.2016.81

Enmozhi, S.K., Raja, K., Sebastine, I. and Joseph, J. (2020) 'Andrographolide as a potential inhibitor of SARS-coV-2 main protease: an in silico approach', *Journal of Biomolecular Structure and Dynamics*, pp.1–7, Advance Online Publication, https://doi.org/10.1080/07391102.2020.1760136

Enmozhi, S.K., Raja, K., Sebastine, I. and Joseph, J. (2020) 'Andrographolide as a potential inhibitor of SARS-CoV-2 main protease: an in silico approach', *Journal of Biomolecular Structure and Dynamics,* doi: 10.1080/07391102.2020.1760136.

Guan, W.J., Ni, Z.Y., Hu, Y., Liang, W.H., Ou, C.Q., He, J.X., Liu, L., Shan, H., Lei, C.L., Hui, D., Du, B., Li, L.J. and Zeng, G., Yuen, K.Y., Chen, R.C., Tang, C.L., Wang, T., Chen, P.Y., Xiang, J., Li, S.Y., Wang, J.L., Liang, Z.J., Peng, Y.X., Wei, L., Liu, Y., Hu, Y.H., Peng, P., Wang, J.M., Liu, J.Y., Chen, Z., Li, G., Zheng, Z.J., Qiu, S.Q., Luo, J., Ye, C.J., Zhu, S.Y., Zhong, N.S. (2020) 'Clinical characteristics of coronavirus disease 2019 in China. China medical treatment expert group for Covid-19', *The New England Journal of Medicine*, Advance Online Publication, https://doi.org/10.1056/NEJMoa2002032

Guo, Y., Cao, Q., Hong, Z., Tan, Y., Chen, S., Jin, H., Tan, K., Wang, D. and Yan, Y. (2020) 'The origin, transmission and clinical therapies on coronavirus disease 2019 (COVID-19) outbreak – an update on the status', *Military Medical Research*, Vol. 7, No. 1, p.11, https://doi.org/10.1186/s40779-020-00240-0

Hanwell, M.D., Curtis, D.E., Lonie, D.C., Vandermeersch, T., Zurek, E. and Hutchison, G.R. (2012) 'Avogadro: An advanced semantic chemical editor, visualization, and analysis platform', *J. Cheminform*, Vol. 4, p.17, https://doi.org/10.1186/1758-2946-4-17

Husain, A., Ahmad, A., Khan, S.A., Asif, M., Bhutani, R. and Al-Abbasi, F.A. (2016) 'Synthesis, molecular properties, toxicity and biological evaluation of some new substituted imidazolidine derivatives in search of potent anti-inflammatory agents', *Saudi Pharm. J.*, Vol. 24, pp.104–114.

Jin, Z., Du, X., Xu, Y., Deng, Y., Liu, M., Zhao, Y., Zhang, B., Li, X., Zhang, L., Peng, C., Duan, Y., Yu, J., Wang, L. and Yang, K., Liu, F., Jiang, R., Yang, X., You, T., Liu, X., Yang, X., Bai, F., Liu, H., Liu, X., Guddat, L.W., Xu, W., Xiao, G., Qin, C., Shi, Z., Jiang, H., Rao, Z. and Yang, H. (2020) 'Structure of mpro from COVID-19 virus and discovery of its inhibitors', *Nature*, https://doi.org/10.1038/s41586-020-2223-y

Jorgensen, W.L. (2004) 'The many roles of computation in drug discovery', *Science*, Vol. 303, pp.1813–1818.

Kitchen, D.B., Decornez, H., Furr, J.R. and Bajorath, J. (2004) 'Docking and scoring in virtual screening for drug discovery: methods and applications', *Nat. Rev. Drug Discov.*, Vol. 3, pp.935–949.

Langer, T. and Hoffmann, R.D. (2001) 'Virtual screening: an effective tool for lead structure discovery?', *Curr. Pharm. Des*., Vol. 7, pp.509–527.

Lee, S.K., Lee, I.H., Kim, H.J., Chang, G.S., Chung, J.E. and No, K.T. (2003) *The PreADME Approach: Web-Based Program for Rapid Prediction of Physicochemical, Drug Absorption and Drug-Like Properties, Euro QSAR 2002 Designing Drugs and Crop Protectants: Processes, Problems and Solutions*, Blackwell Publishing Maldenh, USA, pp.418–420.

Lipinski, C.A., Lombardo, F., Dominy, B.W. and Feeney, P.J. (2001) 'Experimental and computational approaches to estimate solubility and permeability in drug discovery and development settings', *Adv. Drug. Deliver Rev*., Vol. 23, pp.4–25.

Mcconkey, B., Sobolev, V. and Edelman, M. (2002) 'The performance of current methods in ligand-protein docking', *Curr Sci.*, Vol. 83, No. 7, pp.845–856.

Molegro Molecular Viewer. MMV 2.5.0 (2012) *CLC Bio*, Qiagen Inc.

Morris, G.M., Huey, R., Lindstrom, W., Sanner, M.F., Belew, R.K., Goodsell, D.S. and Olson, A.J. (2009) 'AutoDock4 and AutoDockTools4: Automated docking with selective receptor flexibility', *J. Computational Chemistry*, Vol. 16, pp.2785–2791.

Pillaiyar, T., Manickam, M., Namasivayam, V., Hayashi, Y. and Jung, S.H. (2016) 'An overview of severe acute respiratory syndrome-coronavirus (SARS-CoV) 3CL protease inhibitors: peptidomimetics and small molecule chemotherapy', *Journal of Medicinal Chemistry*, Vol. 59, pp.6595–6628, https://doi.org/10.1021/acs.jmedchem.5b01461

Rastogi, S.C., Mmendiratta, N. and Rastogi, P. (2015) 'Bioinformatics methods and applications genomics, proteomics and drug discovery', *Structural Biology and Virtual Screening for Drug Discovery*, 4th ed., PHL Learning Private Limited, Delhi, pp.426–444.

Rothe, C., Schunk, M., Sothmann, P., Bretzel, G., Froeschl, G., Wallrauch, C., Zimmer, T., Thiel, V., Janke, C. and Guggemos, W., Seilmaier, M., Drosten, C., Vollmar, P., Zwirglmaier, K., Zange, S., Wolfel, R. and Hoelscher, M. (2020) 'Transmission of 2019-nCoV infection from anasymptomatic contact in Germany', *New England Journal of Medicine*, Vol. 382, No. 10, pp.970–971, https://doi.org/10.1056/NEJMc2001468

Sanner, M.F. (1999) 'Python: A programming language for software integration and development', *J. Mol. Graph Mod.*, Vol. 17, No. 1, pp.57–61.

Situation Report – 152 (2020) *Coronavirus Disease 2019 (COVID-19)*, World Health Organization, https://www.who.int/docs/default-source/coronaviruse/situation-reports/20200620-covid-19-sitrep-152.pdf?sfvrsn=83aff8ee_2

Tamargo, J., Le Heuzey, J.Y. and Mabo, P. (2015) 'Narrow therapeutic index drugs: a clinical pharmacological consideration to flecainide', *European Journal of Clinical Pharmacology*, Vol. 71, No. 5, pp.549–567, https://doi.org/10.1007/s00228-015-1832-0

Wang, D., Hu, B., Hu, C., Zhu, F., Liu, X., Zhang, J., Wang, B., Xiang, H., Cheng, Z., Xiong, Y., Zhao, Y., Li, Y. and Wang, X., Peng, Z. (2020) 'Clinical characteristics of 138 hospitalized patients with 2019 novel coronavirus–infected pneumonia in Wuhan, China', *JAMA*, Vol. 323, No. 11, p.1061, https://doi.org/10.1001/jama.2020.1585

Wu, F., Zhao, S., Yu, B., Chen, Y.M., Wang, W., Song, Z.G., Hu, Y., Tao, Z.W., Tian, J.H., Pei, Y.Y., Yuan, M.L., Zhang, Y.L., Dai, F.H., Liu, Y., Wang Q.M., Zheng, J.J., Xu, L., Holmes, E.C. and Zhang Y.Z. (2020) 'A new coronavirus associated with human respiratory disease in China', *Nature*, Vol. 579, pp.265–269, https://doi.org/10.1038/s41586-020-2008-3

Yang, H., Yang, M., Ding, Y., Liu, Y., Lou, Z., Zhou, Z., Sun, L., Mo, L., Ye, S., Pang, H., Gao, G.F., Anand, K., Bartlam, M., Hilgenfeld, R. and Rao, Z. (2003) 'The crystal structures of severe acute respiratory syndrome virus main protease and its complex with an inhibitor', *Proc Natl Acad Sci, U.S.A*, Vol. 100, No. 23, p.13190-13195, doi: 10.1073/pnas.1835675100.

Zhou, P., Yang, X.L., Wang, X.G., Hu, B., Zhang, L., Zhang, W., Si, H.R., Zhu, Y., Li, B., Huang, C.L., Chen, H.D., Chen, J., Luo, Y., Guo, H., Jiang, R.D., Liu, M.Q., Chen, Y., Shen, X.R., Wang, X., Zheng, X.S., Zhao, K., Chen, Q.J., Deng, F., Liu, L.L., Yan, B., Zhan, F.X., Wang, Y.Y., Xiao, G.F. and Shi, Z.L. (2020) 'A pneumonia outbreak associated with a new coronavirus of probable bat origin', *Nature*, Vol. 579, pp.270–273, https://doi.org/10.1038/s41586-020-2012-7

Graphical abstract